HGG Advances

REPORT

Biallelic variants in *TAMM41* are associated with low muscle cardiolipin levels, leading to neonatal mitochondrial disease

Kyle Thompson,[1] Lucas Bianchi,[2] Francesca Rastelli,[1] Florence Piron-Prunier,[3] Sophie Ayciriex,[4] Claude Besmond,[2] Laurence Hubert,[2] Magalie Barth,[5] Inês A. Barbosa,[6] Charu Deshpande,[7] Manali Chitre,[8] Sarju G. Mehta,[8] Eric J.M. Wever,[9,10,11] Pascale Marcorelles,[12] Sandra Donkervoort,[13] Dimah Saade,[13] Carsten G. Bönnemann,[13] Katherine R. Chao,[14] Chunyu Cai,[15] Susan T. Iannaccone,[15] Andrew F. Dean,[8,16] Robert McFarland,[1,17] Frédéric M. Vaz,[9,11,18] Agnès Delahodde,[3] Robert W. Taylor,[1,17] and Agnès Rötig[2,*]

Summary

Mitochondrial disorders are clinically and genetically heterogeneous, with variants in mitochondrial or nuclear genes leading to varied clinical phenotypes. *TAMM41* encodes a mitochondrial protein with cytidine diphosphate-diacylglycerol synthase activity: an essential early step in the biosynthesis of phosphatidylglycerol and cardiolipin. Cardiolipin is a mitochondria-specific phospholipid that is important for many mitochondrial processes. We report three unrelated individuals with mitochondrial disease that share clinical features, including lethargy at birth, hypotonia, developmental delay, myopathy, and ptosis. Whole exome and genome sequencing identified compound heterozygous variants in *TAMM41* in each proband. Western blot analysis in fibroblasts showed a mild oxidative phosphorylation (OXPHOS) defect in only one of the three affected individuals. In skeletal muscle samples, however, there was severe loss of subunits of complexes I–IV and a decrease in fully assembled OXPHOS complexes I–V in two subjects as well as decreased TAMM41 protein levels. Similar to the tissue-specific observations on OXPHOS, cardiolipin levels were unchanged in subject fibroblasts but significantly decreased in the skeletal muscle of affected individuals. To assess the functional impact of the *TAMM41* missense variants, the equivalent mutations were modeled in yeast. All three mutants failed to rescue the growth defect of the *Δtam41* strains on non-fermentable (respiratory) medium compared with wild-type *TAM41*, confirming the pathogenicity of the variants. We establish that *TAMM41* is an additional gene involved in mitochondrial phospholipid biosynthesis and modification and that its deficiency results in a mitochondrial disorder, though unlike families with pathogenic *AGK* (Sengers syndrome) and *TAFAZZIN* (Barth syndrome) variants, there was no evidence of cardiomyopathy.

Mitochondrial membranes have a unique lipid composition with low phospholipid to protein and sterol to protein ratios compared with other subcellular fractions and a high cardiolipin (CL) content in the range of 10%–15%.[1] Mitochondria are able to synthesize some of their own lipids, phosphatidylethanolamine (PE), phosphatidic acid (PA), phosphatidylglycerol (PG), and CL. CL is an acidic mitochondrial lipid that consists of three glycerol molecules bridged by two phosphates where the outer two glycerol moieties carry a total of four fatty-acid side chains. One of the key functions of CL is the mediation of protein interactions in the inner mitochondrial membrane (IMM), which in turn influences a diverse range of central processes, such as respiratory chain biogenesis, stabilization of respiratory chain supercomplexes, mitochondrial dynamics, iron-sulfur cluster (Fe-S) biogenesis, and mitophagy. CL also is involved in the mitochondrial protein import machinery, for example, the assembly of TIM23 with the presequence translocase-associated motor (PAM) complex dependents on CL, and more recently, CL has

[1]Wellcome Centre for Mitochondrial Research, Clinical and Translational Research Institute, Faculty of Medical Sciences, Newcastle University, Newcastle Upon Tyne NE2 4HH, UK; [2]INSERM UMR1163, Université Paris Cité, Institut Imagine, 75015 Paris, France; [3]Université Paris-Saclay, CEA, CNRS, Institute for Integrative Biology of the Cell (I2BC), 91198 Gif-sur-Yvette, France; [4]Univ Lyon, CNRS, Université Claude Bernard Lyon 1, Institut des Sciences Analytiques, UMR 5280, 5 rue de la Doua, 69100 Villeurbanne, France; [5]Service de Génétique, Centre Hospitalier Universitaire Angers, Angers, France; [6]Division of Genetics and Molecular Medicine, King's College London School of Medicine, Guy's Hospital, London SE1 9RT, UK; [7]Clinical Genetics Unit, Guys and St. Thomas' NHS Foundation Trust, London SE1 9RT, UK; [8]Cambridge University Hospitals NHS Foundation Trust, Cambridge CB2 0QQ, UK; [9]Laboratory Genetic Metabolic Diseases, Amsterdam UMC, University of Amsterdam, Departments of Clinical Chemistry and Pediatrics, Amsterdam Gastroenterology Endocrinology Metabolism, 1105 AZ Amsterdam, the Netherlands; [10]Bioinformatics Laboratory, Department of Epidemiology & Data Science, Amsterdam Public Health research institute, 1100 DE Amsterdam UMC, University of Amsterdam, the Netherlands; [11]Core Facility Metabolomics, Amsterdam UMC, 1105 Amsterdam, the Netherlands; [12]Department of Pathology, EA4586 LIEN Université de Brest, CHRU Brest, 29609 Brest, France; [13]National Institute of Neurological Disorders and Stroke, National Institutes of Health, Bethesda, MD 20892, USA; [14]Center for Mendelian Genomics, Program in Medical and Population Genetics, Broad Institute of MIT and Harvard, Cambridge, MA 02142, USA; [15]Departments of Pediatrics and Neurology, University of Texas Southwestern Medical Center, Dallas, TX 75390, USA; [16]Department of Histopathology, Cambridge University Hospital NHS Foundation Trust, Cambridge, UK; [17]NHS Highly Specialised Service for Rare Mitochondrial Disorders of Adults and Children, Newcastle Upon Tyne Hospitals NHS Foundation Trust, Newcastle Upon Tyne NE1 4LP, UK; [18]Department of Pediatrics, Emma Children's Hospital, Amsterdam UMC, University of Amsterdam, 1105 AZ Amsterdam, the Netherlands

*Correspondence: agnes.rotig@inserm.fr

https://doi.org/10.1016/j.xhgg.2022.100097.

Table 1. Clinical feature of subjects with biallelic *TAMM41* variants

	Subject 1	Subject 2	Subject 3
Sex	F	F	F
Age of onset	at birth	at birth	at birth
Onset symptom	lethargy	lethargy, hypotonia	lethargy
Age	7 years	8 years	died at 3 months
Birth weight	2.8 kg	3.2 kg	3.4 kg
Delivery	41 + 4 weeks normal vaginal delivery	39 weeks C-section for breech presentation	39 weeks normal vaginal delivery
Motor skills	rolling on back, head drop 6 months, unable to walk, wheelchair bound	head control at 3 months, sitting independently at 6 months, walked independently at 13 months	no contact (3 months)
Social and intellectual	normal	ADHD and dyslexia, in 6th grade with an individualized learning plan	
Brain MRI	normal at 2 years		
Neuromuscular symptoms			
Myopathy	proximal and distal	proximal	
Hypotonia	yes	yes	yes
Reflexes	areflexia	areflexia	
Ptosis	yes	yes	yes
PEO	yes	no	
Swallow	dysphagia		swallowing difficulties

ADHD, attention deficit hyperactivity disorder.

been found to mediate the association of the TIM23 complex with its integral membrane subunit, TIMM50.[2]

CL is synthesized on the matrix side of the IMM. *TAMM41* (MIM: 614948; mitochondrial translocator assembly and maintenance homolog 41) encodes a phosphatidate cytidylyltransferase (CDP-DAG synthase), the first mitochondrial enzyme of CL biosynthesis pathway, that converts PA and cytidine triphosphate (CTP) into cytidine diphosphate (CDP)-diacylglycerol (CDP-DAG).[3] CDP-DAG is then converted to phosphatidylglycerol phosphate, which is dephosphorylated to form PG. CL synthase then condenses PG and CDP-DAG to form CL. A CL phospholipase and the transacylase, tafazzin, are subsequently required to produce the mature fatty acid composition of CL via deacylation and reacylation remodeling.[4]

In humans, the only genetic disease related to a CL biosynthesis and remodeling defect is Barth syndrome (MIM: 302060), caused by variants in *TAFAZZIN* (MIM: 300394), which encodes tafazzin.[5] Barth syndrome, an X-linked disease, is clinically characterized by cardioskeletal myopathy and neutropenia associated with mitochondrial dysfunction.[6] Tafazzin transfers acyl chains from various phospholipids to monolyso-CL (MLCL) via transacylation, and deleterious variants in *TAFAZZIN* are associated with a CL profile that contains more saturated acyl chains and increased MLCL levels.[7] Here, we describe the identification by whole-exome sequencing (WES) and whole-genome sequencing (WGS) of a novel cause of CL biosynthesis defect related to variants in *TAMM41* in three unrelated families of various ethnic origins.

Our study adhered to the Declaration of Helsinki and was approved by the Institutional Review Boards at each site. Written informed consent was obtained from the respective parents of each subject. The three independent subjects were matched using the online GeneMatcher platform.[8]

Subject 1 is an 11-year-old girl born to non-consanguineous parents of European descent (birth weight: 2.8 kg). She presented with failure to thrive and lethargy from birth (Table 1). She was admitted to pediatric intensive care at 5 weeks due to aspiration pneumonia, requiring intubation and intravenous antibiotics followed by percutaneous endoscopic gastrostomy insertion for unsafe swallow. She exhibited development delay in her gross motor skills; she was sitting unsupported at the age of 5 years but remained unable to walk and was wheelchair bound. She has profound hypotonia and myopathy, which is worse in the proximal muscle groups of the neck, trunk, shoulders, and hips. She has chronic progressive external ophthalmoplegia (CPEO) and bilateral ptosis. She also exhibits mild dysmorphic facial features suggestive of myopathic disease, with a long narrow face and tented mouth. She also presented with recurrent infections that could be related to autosomal dominant chronic mucocutaneous candidiasis inherited from the mother; both subject 1 and her mother are heterozygous for a c.820C>T

Table 2. OXPHOS complex enzyme activities in muscle

	Muscle homogenate		Fibroblasts (nmol/min/mg prot)
	S1 (ratio to CS activity)	S3 (nmol/min/mg prot)	S3
CI	0.089 (0.104–0.268)	7 (30–100)	233 (100–270)
CII		38 (30–130)	67 (30–80)
CIII		97 (195–500)	642 (140–327)
CII + III	0.091 (0.040–0.204)		
CIV	0.008 (0.014–0.034)	78 (200–400)	729 (295–665)

Reference values are shown in parentheses. OXPHOS measurement on muscle homogenate has been done in two different labs using different reference ranges. CI, NADH ubiquinol reductase; CII, succinate ubiquinol reductase; CIII, ubiquinol cytochrome *c* reductase; CII + III, succinate cytochrome *c* reductase; CIV, cytochrome *c* oxidase; CS, citrate synthase.

(p.Arg274Trp) *STAT1* variant reported as pathogenic in ClinVar (ClinVar: RCV001090650.1). Brain magnetic resonance imaging (MRI), electromyography, and lumbar puncture have been normal though creatinine kinase (CK) has been elevated (407 U/I). Initially, methylmalonic acid (MMA) was markedly increased (689 mol/mmol [0–20]) with accompanying mild increase in methylcitrate. Lactic aciduria and ketonuria were also noted. B12 therapy was initiated, and the MMA improved, but lactic aciduria and ketonuria persisted with a dicarboxylic/3-hydroxycarboxylic response. A moderate increase in 3-methylglutaconate was also noted on this sample. At other times, citric acid cycle intermediates were identified in the urine. Diagnostic muscle biopsy revealed minor variation in fiber size, some basophilically stippled fibers, and rare instances of regeneration. No neurogenic features, necrosis, inflammation, vacuolation, ragged-red fibers, or excess sarcoplasmic lipid droplets were observed. The majority of fibers exhibited sparse punctate staining with cytochrome oxidase (COX) and succinate dehydrogenase (SDH), with some fibers being entirely negative for oxidative stains (Figure S1). Respiratory chain analysis showed decreased activities of complexes I and IV (Table 2). No abnormality of mtDNA variation, deletion, or depletion could be detected.

Subject 2 is a now 12-year-old girl born to non-consanguineous white American parents. She was hypotonic, but not lethargic, at birth. She developed normally and walked independently at 14 months of age (Table 1). She presented with proximal muscle weakness, predominantly affecting the neck muscles at the age of 2 years. She had bilateral ptosis, normal extraocular movements, dysmorphic facial features secondary to myopathic facial weakness, and bilateral ankle contractures. CK was moderately elevated (646 U/l). She was negative for acetylcholine esterase receptor antibody, which is a marker of myasthenia gravis. Nerve conduction studies of the ulnar and facial motor nerves were normal. Skeletal muscle biopsy showed type I predominance, excessive fiber size variability in both type I and type II fibers, and scattered regenerating fibers. There were frequent scattered COX-deficient fibers that were also pale on SDH stain. No ragged-red fibers were present on Gömöri trichrome. Electron microscopy showed that mitochondria were normal in distribution and morphology (Figure S1). 3-methylglutaconic aciduria testing and oxidative enzyme activity measurements were not performed.

Subject 3 was a girl born to non-consanguineous parents of European descent at 39 weeks through normal vaginal delivery and weighed 3.4 kg (Table 1). She was lethargic from birth and developed bilateral ptosis and dysphagia in the 1st week of life. She was fed parenterally from 2 months old due to severe gastroesophageal reflux. She did not fix and follow objects with her eyes. She died from respiratory failure at the age of 3 months. She had normal blood lactate and urine organic acids. Enlarged mitochondria with irregular shape and increased lipid droplets were observed by electron microscopy (Figure S1). Respiratory chain enzyme analysis in skeletal muscle revealed decreased activities of complexes I, III, and IV, although these were normal in subject fibroblasts (Table 2). There was no evidence of mtDNA depletion in muscle.

Molecular genetic investigations were undertaken for all three subjects using EDTA-blood DNA samples. WES and WGS were performed on subjects 1–3 as family trio. WES (subjects 1 and 3) or WGS (subject 2) data were interpreted according to American College of Medical Genetics (ACMG) guidelines.[9] The pathogenic variants were selected after filtering against known SNPs reported in dbSNP, 1000 Genomes, Exome Variant Server, in-house polymorphisms, and intergenic variants. This filtering resulted in the identification of compound heterozygous variants in *TAMM41* (NM_001284401.1) in each affected individual. All variants were confirmed by Sanger sequencing and all variants segregated with disease in each family following a recessive pattern of inheritance. Subject 1 was compound heterozygous for a c.410C>T (p.Pro137Leu) missense variant and a c.709−2A>G variant in intron 5 and is predicted to affect the acceptor splice site of exon 6 (Table 3). Subject 2 was compound heterozygous for c.256T>C (p.Ser86Pro) missense change and c.411+1G>T in intron 3, predicted to affect splicing of exon 3 (Table 3). Subject 3 was compound heterozygous

Table 3. Evidence of pathogenicity associated with human *TAMM41* variants

	S1		S2		S3	
Nucleotide (NM_001284401.1)	c.410C>T	c.709−2A>G	c.411+1G>T	c.256T>C	c.329A>G	c.806dup
Nucleotide (genomic)	chromosome 3: g.11839223G>A	chromosome 3: g.11809684T>C	chromosome 3: g.11839221C>A	chromosome 3: g.11844091A>G	chromosome 3: g.11839304T>C	chromosome 3: g.11809585dup
dbSNP	rs775491404	rs934260435	rs780204589	rs199871047		rs768826552
Allele	paternal	maternal	paternal	maternal	paternal	maternal
Amino acid	p.Pro137Leu			p.Ser86Pro	p.Tyr110Cys	p.Asn269Lysfs*14
CAAD	33	34	34	13	28.2	24.7
SIFT	0			0.12	0	
PolyPhen	1			0.02	1	
MutationTaster	disease causing (p value: 1)			polymorphism (p value: 1)	disease causing (p value: 1)	
gnomAD allele frequency (all)	G: 0.00001315	G: 0.00003946	T: 0	G: 0.00006570	T: 0	AA: 0
Splicing predictions		MaxEnt: −100.0%; NNSPLICE: −100.0%; HSF: −100.0%	MaxEnt: −100.0%; NNSPLICE: −100.0%; HSF: −100.0%			MaxEnt: 0.0%; NNSPLICE: 0.0%; HSF: −7.9%

for a c.329A>G (p.Tyr110Cys) missense change and a c.806dup (p.Asn269Lysfs*14) variant (Table 3). Tyr110Cys and Pro137Leu affect highly evolutionary conserved amino acids and are predicted to be deleterious, whereas Ser86Pro modified a weakly conserved amino acid (Figure 1A; Table 3). RT-PCR analysis of *TAMM41* RNA extracted from cultured skin fibroblasts showed that the c.709−2A>G variation results in absence of exon 5 in subject 1 and that the c.411+1G>T variation of subject 2 induces absence of exon 3. In subject 3, c.806dup of maternal allele results in a frameshift. Moreover, this also showed in subjects 1 and 3 a higher proportion of the alleles carrying the missense variant, suggesting that c.709−2A>G and c.806dup, from subjects 1 and 3, respectively, result in unstable transcripts. Surprisingly, the paternal allele carrying the c.411+1G>T variation in subject 2 was proportionally higher than the maternal allele, suggesting that the c.256T>C variant induces instability of the transcript (Figure S2). The *TAMM41* variants reported here have been submitted to the ClinVar database (ClinVar: SUB10296292).

To visualize the location of mutant amino acids, we used the AlphaFold machine learning algorithm that predicts protein structures and that has high confidence in the locations of the identified missense variants.[10] In parallel, we also referred to the crystal structure of *S. pombe TAM41*[11] that has previously allowed to identify functional domains of the protein. The three affected amino acids are located in the NTase domain of the protein (Figure 1B). Tyr110 and Pro137 are adjacent to Lys109 and Lys136 CTP binding sites, respectively, and located in the CTP binding pocket formed by Arg133, Lys136, Thr199, and Asn208 that is also predicted to be the active site of the enzyme (Figure 1B).[11] Ser86 is predicted by AlphaFold to be involved in hydrogen bonding (H bonds) with Asn90 (Figure 1C). Tyr110 of the human TAMM41 protein is predicted by AlphaFold to be involved in H bonds with Phe20, Asn65, and Asn98 (Figure 1D). Pro137 is predicted by AlphaFold to be involved in an H bond with Arg133 (Figure 1E). Replacement of this proline, a hydrophobic residue known to bend protein structures, will probably affect the structure of the protein and possibly modify the enzyme activity.

SDS-PAGE and western blot analysis performed on total protein revealed decreased steady-state TAMM41 levels in skeletal muscle of subjects 1 and 2 compared with controls (Figure 2A), suggesting that *TAMM41* variants affect the stability of *TAMM41* cDNA and/or protein. Moreover, a severe decrease of various OXPHOS subunits, including NDUFB8 (complex I), SDHA (complex II), UQCRC2 (complex III), and COXI (complex IV), was observed in muscle of subjects 1 and 2 with a relative sparing of complex V subunit, ATP5A (Figure 2B). No muscle sample of subject 3 was available for western blot analysis. Unfortunately, steady-state levels of TAMM41 could not be assessed in fibroblasts samples, as the anti-TAMM41 antibody resulted in detection of weak and non-specific signal in fibroblast whole-cell lysates (data not shown). A mild decrease in NDUFB8 and COXI subunits was observed in fibroblasts from subject 1 compared with controls (Figure 2D); however, no obvious changes in OXPHOS subunits in fibroblasts from subjects 2 or 3 were detected. These data strongly suggest that there is a tissue-specific manifestation of phenotype due to *TAMM41* variants, with severe consequences in skeletal muscle, but not in fibroblasts.

Blue native PAGE (BN-PAGE) analyses revealed a marked decrease in the assembly of OXPHOS complexes I–IV in muscle of subjects 1 and 2, consistent with the decreased

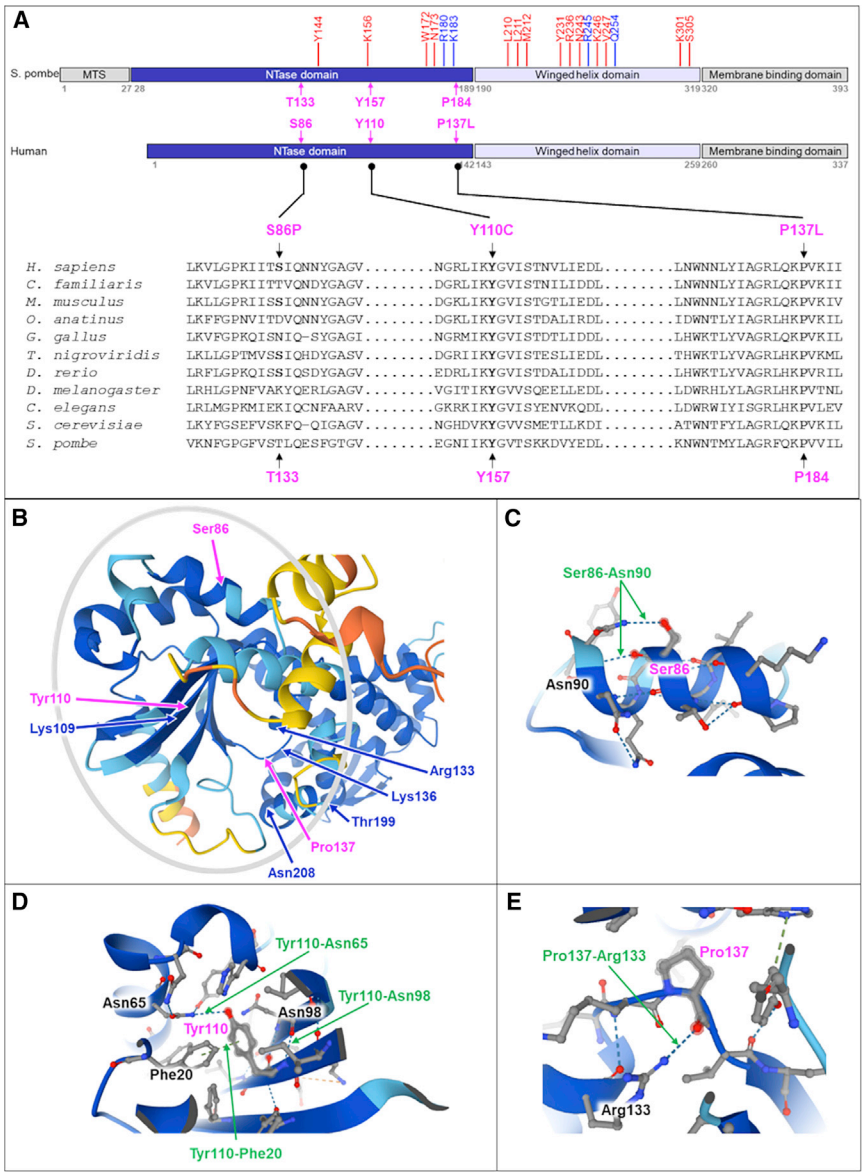

Figure 1. Identification of *TAMM41* variants

(A) Domain architecture of *S. pombe*[11] and human TAMM41 and sequence alignment of TAMM41 proteins from various species. NTase and winged helix domains are in dark and light blue, respectively. MTS, mitochondrial targeting sequence. The amino acid residues involved in CTP binding are shown in blue, and the residues involved in dimer formation are shown in red. The arrows indicate the affected amino acids (pink). Human Ser86, Tyr110, and Pro137 correspond to Thr133, Tyr157, and Pro184 in *S. pombe* and to Lys186, Pro236, and Tyr209 in *S. cerevisiae*.

(B–E) Three-dimensional representation of the human TAMM41 structure predicted by AlphaFold showing the locations and the predictions of hydrogen-bonding (H bond) of mutated amino acids. The mutated residues are highlighted in pink and the H bonds by green arrows. Amino acids in blue correspond to the CTP-binding sites. The gray circle shows the NTase domain. The colors of the 3D structure correspond to the confidence scores of the different parts of the protein (dark blue, very high [pLDDT > 90]; light blue, confident [90 > pLDDT > 70]; yellow, low [70 > pLDDT > 50]; and orange, very low [pLDDT < 50]).

steady-state levels of their subunits (Figure 2C). Complex V assembly was also greatly impaired despite a relatively mild decrease of ATP5A steady-state level detected by western blot. Consistent with the SDS-PAGE experiments, subject fibroblasts samples did not show any obvious defect in the assembly of any of the OXPHOS complexes (Figure 2E), further highlighting a tissue-specific expression of the biochemical phenotype.

To assess the effect of the identified *TAMM41* variants on CL levels, we performed lipidomic analysis as described previously.[12] This demonstrated that, in skeletal muscle, the total CL and PG content was decreased in samples from affected individuals, whereas phosphatidylinositol (PI) and phosphatidylcholine (PC) levels were comparable (Figure 3A). This is consistent with a TAMM41-specific problem, as CL and PG are both synthesized from the mitochondrial pool of CDP-DAG, which is produced via TAMM41, whereas PI is synthesized in the endoplasmic reticulum (ER) and uses CDP-DAG derived from the ER-specific enzymes CDS1 and CDS2.[13] Synthesis of PC is not dependent on CDP-DAG at all. We did not see evidence of an accumulation of PA (not shown), but this is likely due to the fact that the analysis was performed on whole-muscle extracts rather than isolated mitochondria, and PA is also present and can be metabolized in the ER. CDP-DAG was not detected in the lipidomic analysis, since it is metabolized quickly and the absolute steady-state levels are relatively low. Since whole-muscle and fibroblast samples were used for lipidomics, levels of CDP-DAG would also have included ER-derived CDP-DAG and would therefore not be as informative as the downstream, mitochondrial-specific PG and CL levels that were measured. In accordance with the impaired OXPHOS phenotype in muscle of affected individuals and the comparable levels in both control and subject fibroblasts, CL and PG levels in fibroblasts were not decreased in affected individuals (Figure 3B). This reinforces the tissue-specific nature of the defect observed and highlights the correlation between decreased TAMM41, decreased CL levels, and diminished OXPHOS protein levels, which are all observed in skeletal muscle from affected individuals and are suggestive that these

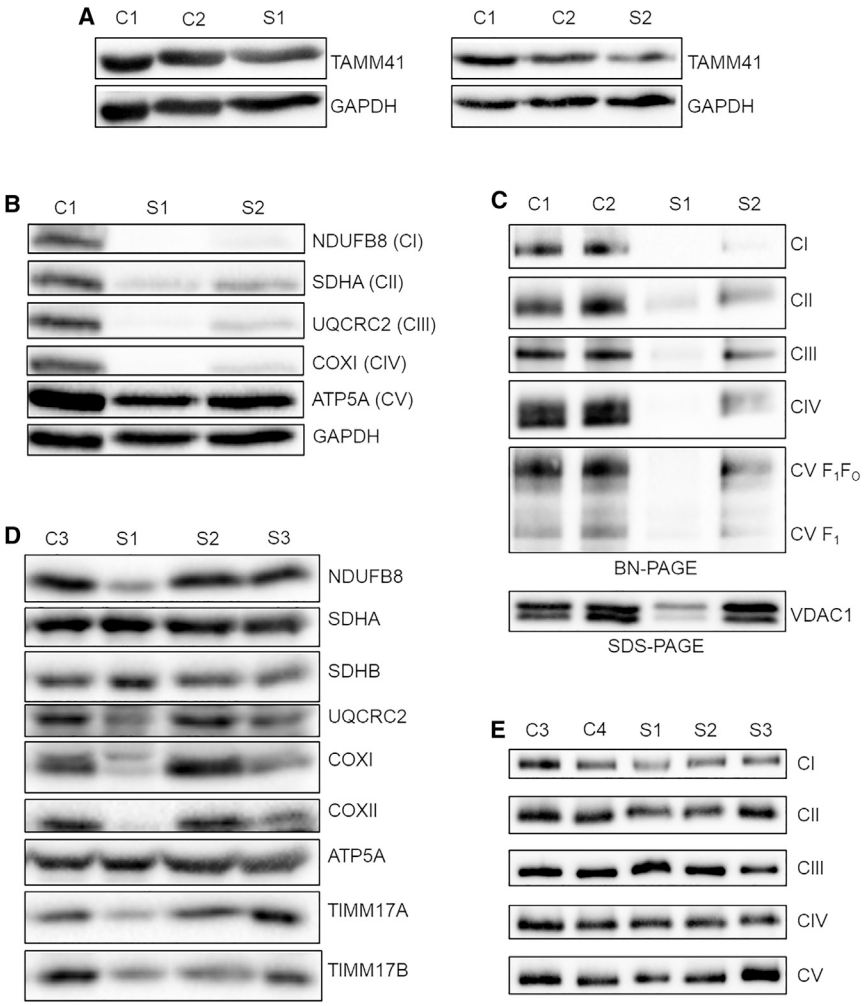

Figure 2. Biochemical investigation of muscle and fibroblasts

(A) Western blot analysis of TAMM41 in skeletal muscle of subjects 1 and 2 (S1 and S2) compared with control individuals (C1 and C2).

(B) Western blot analysis to assess steady-state level of various OXPHOS subunits in skeletal muscle of subjects 1 and 2 (S1 and S2) compared with control individual (C1). GAPDH was used as loading control.

(C) BN-PAGE on skeletal muscle samples from S1 and S2 and control individuals (C1 and C2).

(D and E) Assessment of fibroblasts samples from subjects 1–3 (S1–S3) and control individuals (C3 and C4) by SDS-PAGE (D) and BN-PAGE (E). CI–CV, complex I–V.

TAMM41 variants have a functional consequence leading to the pathology.

To further assess the functional impact of *TAMM41* missense variants, we tested mutant cDNAs for their ability to complement the growth defect in a *Saccharomyces cerevisiae* strain with the *TAM41* gene deleted (*tam41Δ*). Consistent with previous studies,[3,14,15] we observed that *TAM41* is an essential gene in the BY4741 background. Expression of wild-type human *TAMM41* cDNA failed to complement the growth defect of *tam41Δ* yeast strain (not shown), despite a high degree of conservation between yeast and human proteins (40% identity; Figure 1A). We introduced the equivalent various missense variants into the yeast *TAM41* sequence by site-directed mutagenesis and used a plasmid-shuffling system[16] for its expression in *tam41Δ* strain. Growth of the *tam41Δ* strain was fully complemented by wild-type yeast *TAM41* as expected. However, $tam41^{Y209C}$ and $tam41^{P236L}$ variants corresponding to the human Tyr110Cys and Pro137Leu variants, respectively, completely failed to complement the *tam41Δ* growth defect on fermentable media (YPD), especially at 36°C (Figure 4), and on non-fermentable media (YGE and YPG), which renders the cell growth dependent on mitochondrial respiration (Figure 4). Expression of $tam41^{K186P}$ (Ser86Pro in human) rescued growth on fermentable media but only partly complemented the growth on respiratory media particularly at 36°C. Taken together, these results demonstrate the deleterious nature of all subject *TAMM41* missense variants. Moreover, the growth phenotype of the mutant proteins expressed in *tam41Δ* yeast shows a good correlation with the severity of the clinical presentation of the subjects.

We have identified three affected individuals from unrelated families presenting with myopathy, hypotonia, bilateral ptosis, and lethargy associated with compound heterozygous *TAMM41* variants. The unifying clinical features of ptosis, CPEO, and failure to thrive were highly suggestive of a mitochondrial genetic defect. Brain MRI was normal in one subject, and none of them presented with elevated lactate, but respiratory chain analyses within skeletal muscle in two subjects clearly revealed abnormal activities, confirming a biochemical diagnosis of mitochondrial disease. The *TAMM41* variants identified by WES resulted in a relatively mild decrease in steady-state TAMM41 protein levels in skeletal muscle (subjects 1 and 2), leading to disrupted assembly of OXPHOS complexes, a marked decrease in steady-state protein levels of multiple OXPHOS subunits and, consequently, the severe impairment of respiratory chain enzyme activities. In contrast, subject fibroblasts displayed a modest decrease of OXPHOS protein abundance that did not affect mitochondrial respiratory chain enzyme activities. This was mirrored in the results from the quantitative lipidomic analyses, which demonstrated a clear decrease in CL and PG in subject skeletal muscle samples but no matching phenotype in subject fibroblasts.

This tissue-specific effect of the variants is not surprising, as there are many examples of variants causing mitochondrial

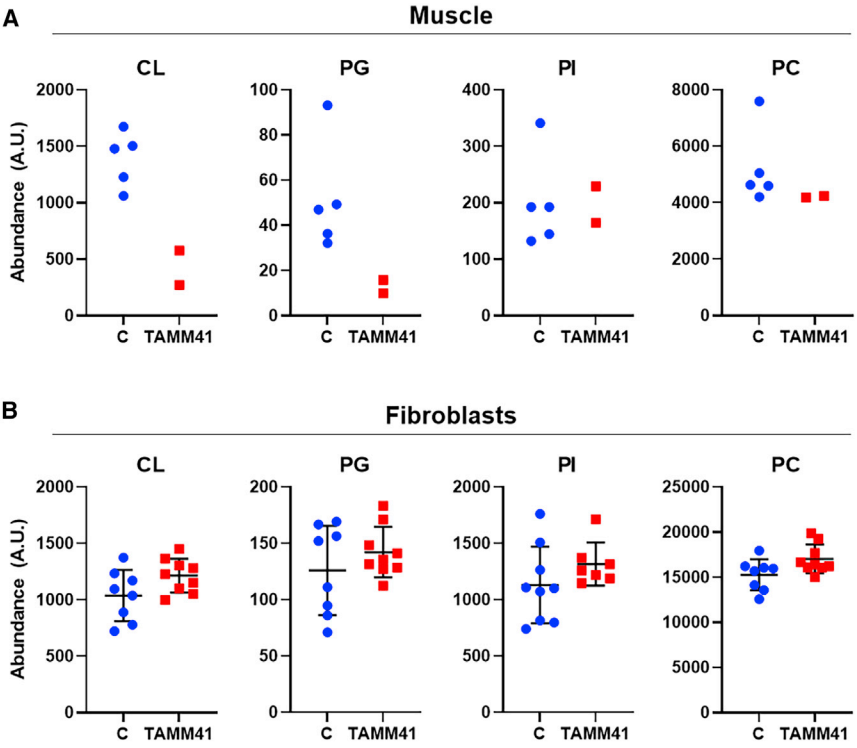

Figure 3. Quantification of cardiolipin (CL), phosphatidylglycerol (PG), phosphatidylinositol (PI), and phosphatidylcholine (PC) species

(A) Total summations of CL, PG, PI, and PC species in muscle of three control individuals (blue circles) and of subjects 1 and 2 (red squares). CL and PG are clearly lower in affected individuals when compared with PI and PC, where levels are comparable in both groups.

(B) Total summations of CL, PG, PI, and PC species in fibroblasts of three control individuals (blue circles) and of subjects 1–3 (red squares). No differences were seen in the levels of all major classes shown. Averages and standard deviations are indicated in black.

disorders that express defects in muscle, but not in fibroblasts. In this case, we show that the OXPHOS deficiency correlates with decreased CL and it is possible that the difference between the two tissues tested could be that fibroblasts are less reliant upon TAMM41 for the CDP-DAG needed to produce CL. There is some evidence to suggest that the ER enzymes CDS2 and CDS2 can contribute toward CL synthesis,

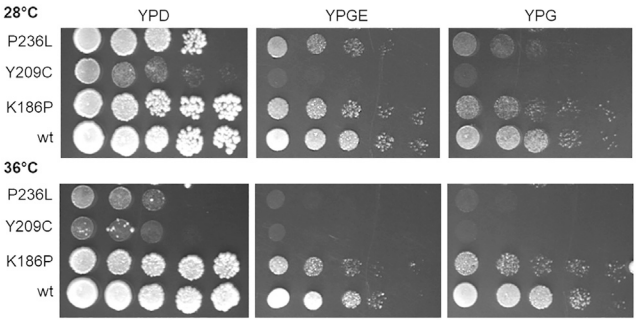

Figure 4. Functional complementation assay of a yeast *tam41Δ*-null mutant

Growth of *tam41Δ* cells was tested either on glucose (YPD), glycerol (YPG), or glycerol + ethanol medium (YPGE). The *tam41Δ* strain containing an *URA3*-plasmid expressing wild-type *TAM41* from its own promoter was transformed with a *LEU2*-plasmid encoding either wild-type *TAM41* or *tam41* mutants under the control of the *TAM41* promoter. After 5-fluoro-orotic acid (5-FOA) treatment to eliminate the *URA3*-plasmid encoding wild-type *TAM41*, cells expressing only wild-type (*TAM41*) or *tam41* mutants were spotted onto YPD, YPG, or YPGE plates. Drop-dilution growth tests were performed at 1/10 dilution steps, and yeast were incubated on YPD for 2 days or YPG or YPGE for 4 days at 28°C or 36°C.

since mouse knockouts of regulatory genes *Ppargc1a*[17] (encoding PGC-1α) or *Prkaa2*[18] (encoding AMPKα2) led to a decrease in CL alongside a decrease in *CDS1* or *CDS2* mRNA, respectively. However, these studies did not assess *TAMM41* mRNA levels as TAMM41, and its CDS activity had not yet been identified. Furthermore, yeast knockouts of *tam41* do have some low levels of CL synthesis, suggesting the yeast *CdsA* may be able to provide some of the CDP-DAG required for CL synthesis.[13] For CDP-DAG produced in the ER to be used for CL synthesis, this would need to be transported from the ER to the inner mitochondrial membrane. No such lipid transporter has yet been identified, but it remains an interesting possibility. In our experiments, we were unable to assess the effects of the variants on TAMM41 protein levels in fibroblasts due to weak and non-specific signal in fibroblast samples (including controls). This contrasted with the strong specific signal in skeletal muscle samples, perhaps suggesting a difference in expression of TAMM41 between the tissues. However, mRNA data available on the GTEX portal (https://gtexportal.org/home/gene/TAMM41) suggests expression of *TAMM41* transcript is actually higher in fibroblasts than in muscle tissue. Post-transcriptional or post-translational modification in fibroblasts could potentially explain the seemingly lower expression of TAMM41 protein in fibroblasts. As with many other mitochondrial disorders, we do not fully understand the reason for the tissue-specific expression of the biochemical and clinical phenotype caused by *TAMM41* variants.

We demonstrate that variants in *TAMM41* represent the second cause of disturbed CL biosynthesis and illustrate the clinical heterogeneity associated with a similar metabolic defect, Barth syndrome, which is caused by variants in *TAFAZZIN*. Barth syndrome is a mitochondriopathy that is mainly characterized by cardiomyopathy and myopathy based on a generalized CL-remodeling defect that is found in several tissues, including fibroblasts. Symptomatically,

TAMM41 deficiency and Barth syndrome have myopathy in common; however, the subjects with TAMM41 deficiency did not display a cardiac phenotype—all subjects had either electrocardiogram or cardio echography performed, which were normal. The lack of CL deficiency and OXPHOS defects in TAMM41-deficient fibroblasts suggests a tissue-specific expression of the biochemical defect that might explain the phenotypic variability of the two disorders in the same biosynthetic pathway. Interestingly, *TAMM41* deletion by CRISPR in zebrafish does lead to abnormal heart development, but this was attributed to TAMM41 participating in PINK1-dependent mitophagy rather than its role in CL synthesis, as CL levels were unchanged in TAMM41-depleted zebrafish heart cell lines.[19]

In summary, this report highlights the importance of lipid homeostasis to sustain normal mitochondrial function and adds to a growing number of lipid biosynthesis defects associated with pathogenic variants in *AGK*, *SERAC1*, and *LIPT2* or numerous genes encoding CoQ_{10} biosynthesis enzymes that result in mitochondrial disease.[20–22]

Data and code availability

The authors confirm that the data supporting the findings of this study are available within the article and/or its supplemental material or can be made available upon reasonable request.

Supplemental information

Supplemental information can be found online at https://doi.org/10.1016/j.xhgg.2022.100097.

Acknowledgments

This study was financially supported by the Agence Nationale de la Recherche through the Investissements d'Avenir program ANR-10-IAHU-01 (A.R., L.B., C.B., and L.H.), the E-Rare project GENOMIT (01GM1207; A.R. and L.B.), the French National Agency for Research (ANR-16-CE16-0025-04; A.D. and F.P.-P.), and the "Association Française contre les Myopathies" (AFM – MITOSCREEN, project no. 17122; A.D. and F.P.-P.). We acknowledge the use of bioresources of the Necker Imagine DNA biobank (BB-033-00065). R.M. and R.W.T. are supported by the Wellcome Trust Centre for Mitochondrial Research (203105/Z/16/Z), the Medical Research Council (MRC) International Center for Genomic Medicine in Neuromuscular Disease (MR/S005021/1), the Mitochondrial Disease Patient Cohort (UK) (G0800674), the UK NIHR Biomedical Research Center for Aging and Age-Related Disease Award to the Newcastle upon Tyne Foundation Hospitals NHS Trust, the Lily Foundation, and the UK NHS Specialist Commissioners, which funds the "Rare Mitochondrial Disorders of Adults and Children" Diagnostic Service in Newcastle upon Tyne. R.W.T. also receives financial support from the Pathology Society. K.T. and I.A.B. were supported by the Lily Foundation. C.G.B. is supported by intramural funds from the NIH National Institute of Neurological Disorders and Stroke. Sequencing and analysis were provided by the Broad Institute of MIT and Harvard Center for Mendelian Genomics (Broad CMG) and was funded by the National Human Genome Research Institute, the National Eye Institute, and the National Heart, Lung, and Blood Institute grant UM1 HG008900 to Daniel MacArthur and Heidi Rehm.

Declaration of interests

The authors declare no competing interests.

Received: October 18, 2021
Accepted: February 25, 2022

Web resources

OMIM, http://www.omim.org/
Alamut Visual, https://www.interactive-biosoftware.com/alamut-visual/
PDB, http://www.rcsb.org/
ClinVar, https://www.ncbi.nlm.nih.gov/clinvar/

References

1. Pennington, E.R., Funai, K., Brown, D.A., and Shaikh, S.R. (2019). The role of cardiolipin concentration and acyl chain composition on mitochondrial inner membrane molecular organization and function. Biochim. Biophys. Acta Mol. Cell Biol. Lipids *1864*, 1039–1052.
2. Martensson, C.U., Doan, K.N., and Becker, T. (2017). Effects of lipids on mitochondrial functions. Biochim. Biophys. Acta Mol. Cell Biol. Lipids *1862*, 102–113.
3. Tamura, Y., Harada, Y., Nishikawa, S., Yamano, K., Kamiya, M., Shiota, T., Kuroda, T., Kuge, O., Sesaki, H., Imai, K., et al. (2013). Tam41 is a CDP-diacylglycerol synthase required for cardiolipin biosynthesis in mitochondria. Cell Metab. *17*, 709–718.
4. Xu, Y., Kelley, R.I., Blanck, T.J., and Schlame, M. (2003). Remodeling of cardiolipin by phospholipid transacylation. J. Biol. Chem. *278*, 51380–51385.
5. Bione, S., D'Adamo, P., Maestrini, E., Gedeon, A.K., Bolhuis, P.A., and Toniolo, D. (1996). A novel X-linked gene, G4.5. is responsible for Barth syndrome. Nat. Genet. *12*, 385–389.
6. DiMauro, S. (2006). Mitochondrial myopathies. Curr. Opin. Rheumatol. *18*, 636–641.
7. Vreken, P., Valianpour, F., Nijtmans, L.G., Grivell, L.A., Plecko, B., Wanders, R.J., and Barth, P.G. (2000). Defective remodeling of cardiolipin and phosphatidylglycerol in Barth syndrome. Biochem. Biophys. Res. Commun. *279*, 378–382.
8. Sobreira, N., Schiettecatte, F., Valle, D., and Hamosh, A. (2015). GeneMatcher: a matching tool for connecting investigators with an interest in the same gene. Hum. Mutat. *36*, 928–930.
9. Richards, S., Aziz, N., Bale, S., Bick, D., Das, S., Gastier-Foster, J., Grody, W.W., Hegde, M., Lyon, E., Spector, E., et al. (2015). Standards and guidelines for the interpretation of sequence variants: a joint consensus recommendation of the American college of medical genetics and Genomics and the association for molecular pathology. Genet. Med. *17*, 405–424.
10. Jumper, J., Evans, R., Pritzel, A., Green, T., Figurnov, M., Ronneberger, O., Tunyasuvunakool, K., Bates, R., Zidek, A., Potapenko, A., et al. (2021). Highly accurate protein structure prediction with AlphaFold. Nature *596*, 583–589.

11. Jiao, H., Yin, Y., and Liu, Z. (2019). Structures of the mitochondrial CDP-DAG synthase Tam41 suggest a potential lipid substrate pathway from membrane to the active site. Structure *27*, 1258–1269.e4.
12. Vaz, F.M., McDermott, J.H., Alders, M., Wortmann, S.B., Kolker, S., Pras-Raves, M.L., Vervaart, M.A.T., van Lenthe, H., Luyf, A.C.M., Elfrink, H.L., et al. (2019). Mutations in PCYT2 disrupt etherlipid biosynthesis and cause a complex hereditary spastic paraplegia. Brain *142*, 3382–3397.
13. Blunsom, N.J., and Cockcroft, S. (2020). CDP-diacylglycerol synthases (CDS): gateway to phosphatidylinositol and cardiolipin synthesis. Front. Cell Dev. Biol. *8*, 63.
14. Gallas, M.R., Dienhart, M.K., Stuart, R.A., and Long, R.M. (2006). Characterization of Mmp37p, a Saccharomyces cerevisiae mitochondrial matrix protein with a role in mitochondrial protein import. Mol. Biol. Cell *17*, 4051–4062.
15. Hazbun, T.R., Malmstrom, L., Anderson, S., Graczyk, B.J., Fox, B., Riffle, M., Sundin, B.A., Aranda, J.D., McDonald, W.H., Chiu, C.H., et al. (2003). Assigning function to yeast proteins by integration of technologies. Mol. Cell *12*, 1353–1365.
16. Boeke, J.D., Trueheart, J., Natsoulis, G., and Fink, G.R. (1987). 5-Fluoroorotic acid as a selective agent in yeast molecular genetics. Methods Enzymol. *154*, 164–175.
17. Lai, L., Wang, M., Martin, O.J., Leone, T.C., Vega, R.B., Han, X., and Kelly, D.P. (2014). A role for peroxisome proliferator-activated receptor gamma coactivator 1 (PGC-1) in the regulation of cardiac mitochondrial phospholipid biosynthesis. J. Biol. Chem. *289*, 2250–2259.
18. Athea, Y., Viollet, B., Mateo, P., Rousseau, D., Novotova, M., Garnier, A., Vaulont, S., Wilding, J.R., Grynberg, A., Veksler, V., et al. (2007). AMP-activated protein kinase alpha2 deficiency affects cardiac cardiolipin homeostasis and mitochondrial function. Diabetes *56*, 786–794.
19. Yang, R.M., Tao, J., Zhan, M., Yuan, H., Wang, H.H., Chen, S.J., Chen, Z., de The, H., Zhou, J., Guo, Y., et al. (2019). TAMM41 is required for heart valve differentiation via regulation of PINK-PARK2 dependent mitophagy. Cell Death Differ. *26*, 2430–2446.
20. Mayr, J.A. (2015). Lipid metabolism in mitochondrial membranes. J. Inherit. Metab. Dis. *38*, 137–144.
21. Habarou, F., Hamel, Y., Haack, T.B., Feichtinger, R.G., Lebigot, E., Marquardt, I., Busiah, K., Laroche, C., Madrange, M., Grisel, C., et al. (2017). Biallelic mutations in LIPT2 cause a mitochondrial lipoylation defect associated with severe neonatal encephalopathy. Am. J. Hum. Genet. *101*, 283–290.
22. Desbats, M.A., Lunardi, G., Doimo, M., Trevisson, E., and Salviati, L. (2015). Genetic bases and clinical manifestations of coenzyme Q10 (CoQ 10) deficiency. J. Inherit. Metab. Dis. *38*, 145–156.